Ming *et al.*
European Journal of Medical Research (2025) 30:95
https://doi.org/10.1186/s40001-025-02350-8

European Journal of Medical Research

RESEARCH Open Access

Long non-coding RNA H19 promotes cervical cancer development via targeting the microRNA-140/ALDH1A1 axis

Jie Ming[1], Fang Cheng[2], Yating Fu[3], Meng Zhang[2], Qian Rou[2], Kaixiong Liu[4], Zinati Nuertai[2], Shanshan Xu[2], Ling Tao[5], Alfira Abudujapar[6] and Ying Liu[2,4*]

Abstract

Background Dysregulation of long non-coding RNA H19 (lncRNA H19) is involved in cervical cancer (CC) progression. This study aims to unveil the specific role and relevant mechanism of lncRNA H19 in CC.

Methods The expression of lncRNA H19 in CC cells was detected by quantitative reverse transcriptase polymerase chain reaction (qRT-PCR). CC cells were transfected with sh-H19, followed by cell proliferation, apoptosis, migration and invasion were examined. After location of H19 in cells using fluorescence in Situ Hybridization (FISH), target microRNAs (miRNAs) and genes associated with lncRNA H19 were predicted using bioinformatics analysis and validated by dual-luciferase reporter assay. Finally, the specific role of lncRNA H19 in CC was explored in vivo.

Results The upregulation of lncRNA H19 was observed in CC cells. LncRNA H19 knockdown inhibited the proliferation, migration, and invasion of CC cells, and remarkably promoted CC cell apoptosis. LncRNA H19 was localized in the nucleus and interacted with miR-140 that was downregulated in CC cells. MiR-140 inhibition reversed the effects of lncRNA H19 knockdown on CC cell development. MiR-140 targets ALDH1A1, and lncRNA H19 knockdown decreased the ALDH1A1 expression, which was rescued by miR-140 inhibition. In vivo experiments also shown that reduction of lncRNA H19 diminishes tumor growth via targeting the miR-140/ALDH1A1 axis.

Conclusion LncRNA H19 promotes the malignant progression of CC through targeting miR-140/ALDH1A1 axis.

Keywords Cervical cancer, Competing endogenous RNA, LncRNA H19, MicroRNA-140, Aldehyde dehydrogenase 1A1

Background

Cervical cancer (CC) is a prominent health burden for women worldwide, ranking fourth of all the other common cancers [1, 2]. An estimated 569,847 new cases of CC and 311,365 deaths occur each year [3]. The 5-year overall survival (OS) rate of CC is 68%, and the average OS of patients with advanced stage is only 16.8 months [4]. Although high diagnostic efficiency of current screening methods such as cytology and human papillomavirus nucleic acid testing for cervical precancerous lesions, and the widespread vaccination of HPV vaccine, the morbidity of CC remains quite high [5]. This highlights the necessity to explore the crucial molecular

*Correspondence:
Ying Liu
lydiasunshine@xjmu.edu.cn
[1] Medical Imaging Center, Affiliated Cancer Hospital of Xinjiang Medical University, Urumqi 830011, Xinjiang, China
[2] Department of Special Needs Comprehensive, Affiliated Cancer Hospital of Xinjiang Medical University, Urumqi 830011, Xinjiang, China
[3] Department of Radiology, Urumqi Stomatological Hospital, Urumqi 830002, Xinjiang, China
[4] Department of Oncology, Bachu County People's Hospital, Bachu 843800, Xinjiang, China
[5] Department of Gynecology, Affiliated Cancer Hospital of Xinjiang Medical University, Urumqi 830011, Xinjiang, China
[6] Affiliated Cancer Hospital of Xinjiang Medical University, Urumqi 830011, Xinjiang, China

mechanisms underlying CC for promoting precision in disease diagnosis and individualized treatment.

It is well known that non-coding RNAs (ncRNAs) account for the vast majority (98%) of human transcripts, which include a wide variety of RNA species, such as microRNAs (miRNAs, ~19–25 nucleotides in length) [6] and long non-coding RNA (lncRNAs, longer than 200 nucleotides) [7]. Moreover, accumulating studies have revealed that lncRNAs function as competing endogenous RNAs (ceRNAs) for miRNAs, thereby impeding the regulation of miRNAs on their target mRNAs [8]. For instance, LINC00861 plays a tumor suppressor role in CC by acting as a ceRNA for miR-513b-5p to target PTEN [9]; lncRNA ACTA2-AS1 accelerates CC progression via up-regulating SMAD3 by sponging miR-143-3p [10]. These findings underscore the potential of studying the regulatory interplay among diverse types of RNAs in CC cells for the development of targeted treatment strategies.

LncRNA H19 is located on chromosome 11 in human and plays a vital role in diverse cancer types [11]. Deregulation of lncRNA H19 is revealed to participate in CC development [12, 13]. Notably, previous studies indicated that lncRNA H19 can interact with miR-140 to modulate the development of ovarian cancer [14] and glioma [15]. In addition, miR-140-3p plays an inhibitory role in CC via targeting RRM2 to inhibit cell proliferation [13], and miR-140-5p impedes the aggressive phenotypes of CC cells by down-regulating FEN1 to induce cell cycle arrest [16]. However, the potential regulatory role of lncRNA H19, acting as a sponge for miR-140 in the CC development, remains largely unexplored.

In a previous study, aldehyde dehydrogenase 1 (ALDH1) was identified as a direct target of miR-140 [17]. ALDH1 are identified as a key regulator during generation and progression in CC [18]. ALDH1A1 is one of the ALDH1 family members, which is up-regulated in CC from precancerous lesions (CIN II–III) [19]. Therefore, we hypothesize that lncRNA H19 could influence CC progression via the miR-140/ALDH1A1 axis.

In this study, our objective was to explore the potential effect of lncRNA H19 on CC progression through the miR-140/ALDH1A1 axis. By doing so, we aimed to uncover a novel mechanism contributing to the pathogenesis of CC, thereby establishing a scientific rationale for the subsequent findings.

Materials and methods

Cell culture

The CC cells, including Hela (SNL-062, SUNNCELL, Hubei, China), Ca-Ski (SNL-067, SUNNCELL, Hubei, China), and C33a (SNL-224, SUNNCELL, Hubei, China), and normal cervical epithelial H8 cells (YS2579, ATCC, Rockville, MD, USA) were cultured in RPMI 1640 (C11875500BT, Gibco, USA) containing 10% fetal bovine serum (FBS, 34080619, Gibco, USA), 100 μg/mL streptomycin, and 100 U/mL penicillin (SV30010, Hyclone, Logan, UT). All these cells were identified by Short Tandem Repeat (STR) profiling. HEK293T cells were cultured in DMEM (Hyclone, Logan, UT) supplemented with 10% FBS, 100 μg/mL streptomycin, and 100 U/mL penicillin. These cells were maintained at 37 °C in an atmosphere of 5% CO_2.

Cell transfection

For down-regulation of lncRNA H19, the sh-H19 sequences (sense sequence: CCTCTAGCTTGGAAA TGAA and antisense sequence: TTCATTTCCAAGCTA GAGG) were obtained in the Designer of Small Interfering RNA website and integrated into pLKO.1 lentiviral vector. To generate high-titer lentivirus, the lentivirus together with the packaging plasmids were co-transfected into HEK293T cells using HighGene transfection reagent (RM09014, ABclonal, Wuhan, China). The multiplicity of infection (MOI) was subsequently determined. Hela and Ca-Ski cells (2×10^5) were seeded into a six-well plate and cultured until they reached a cell density of 70–90%. Hela cells were then infected with lentiviral particles at an MOI of 1×10^8 TU/mL. After 48 h of transfection, cells were harvested.

To further investigate whether lncRNA H19 regulated CC development by modulating miR-140, the lncRNA H19-knockdown Hela cells were further transfected with miR-140 inhibitor (20 μM) or inhibitor negative control (inhibitor NC) synthetized from Sangon Biotech (Shanghai, China) using riboFECT™ CP Reagent (C10502-05, RiboBio, Guangzhou, China). The plates were incubated at the 37 °C, 5% CO_2 incubator for 48 h.

Quantitative reverse transcriptase polymerase chain reaction (qRT-PCR)

Total RNA was extracted using Trizol reagent (15596018, Invitrogen, USA). Total RNA was reversely transcribed into cDNA using the PrimeScriptTM RT Master Mix Kit (RR036A, Takara, Japan). The expression of lncRNA H19, miR-140, and ALDH1A1 was measured with qRT-PCR reaction containing SYBR Green PCR Master Mix (A4004M, Lifeint, Xiamen, China). Table 1 listed the sequence of primers for gene amplification. Relative expression of target genes was determined using the $2^{-\Delta\Delta CT}$ method [20].

CCK-8 assay

Hela and Ca-Ski cells at logarithmic growth stage were collected, digested, and re-suspended with fresh complete medium. Cell suspension was inoculated into the

Table 1 The sequence of primers for gene amplification

Primers	Forward (5′–3′)	Reverse (5′–3′)
LncRNA H19	CAAAGCCTCCACGACTCTGT	TGGGGCGTAATGGAATGCTT
miR-140	CTGTGTCCTGCCAGTGGT TTT	CGGTATCCTGTCCGTGGTTCT
ALDH1A	CGTGGCGTACTATGGATGCT	GACTCCTGGGGTCAGAGGAT
GAPDH	GAGAAGGCTGGGGCT CATTT	AGTGATGGCATGGACTGTGG
U6	AAGACAGCGCAGAATCAC CC	CTCACCAGATGCCCGTTGTA

96-well plate, and the plate was cultured for 48 h in a 37 °C, 5% CO_2 incubator. Then, CCK-8 solution (10 μL, C0037, Beyotime, Jiangsu, China) was added into each well. The plate was incubated in the 37 °C, 5% CO_2 incubator for 2 h, and the absorbance value at 450 nm wavelength was then determined using a micro-plate reader (DR-3518G, Wuxi Hiwell Diatek, China).

Colony formation assay

Hela and Ca-Ski cells (200 cell/well) were inoculated into the 6-well plate and cultured in a 37 °C, 5% CO_2 incubator for 7 days. When visible clones appeared, absolute methanol was added to fix cells for 15 min, and appropriate amount of crystal violet (C0121, Beyotime, Jiangsu, China) was used to stain cells for 20 min. After removing excess dye, the colonies in the ix-well plate were photographed and counted.

Cell apoptosis detection by flow cytometry

After cultured at 37 °C for 24 h, Hela and Ca-Ski cells were digested with 0.25% pancreatin without EDTA and then collected. Cells (5×10^4 cells) were lightly re-suspended with 195 μL Annexin V-EGFP binding solution and double stained with 5 μL Annexin V-EGFP and 10 μL propidium iodide for 15 min in the dark. The percentage of apoptotic cells was detected with a flow cytometry (CytoFLEX S, Beckman Coulter, Fullerton, CA).

Scratch wound healing assay

The migration abilities of Hela cells at 0 and 24 h were assessed by scratch wound healing assay. Briefly, a marker pen was used to draw lines on the back of the 6-well plates. Hela and Ca-Ski cells ($5\times l0^5$) were seeded into the 6-well plates. The next day, cells formed a confluent monolayer, and a "scratch" of the cell monolayer that was perpendicular to the back lines was created using a pipet tip. The scratched cells were discarded via rinsing three times with PBS, and the serum-free medium was added. The plates were incubated in a 37 °C, 5% CO_2 incubator. The scratch wound healing was photographed at 0 and 24 h.

Transwell assay for measuring cell invasion

The upper compartment surface of the bottom membrane of Transwell chamber (Millipore, Billerica, MA, USA) was coated with Matrigel for 4 h at 37 °C. Hela and Ca-Ski cells were digested and re-suspended with serum-free medium. The upper and lower layers of Transwell chambers were, respectively, added with cell suspension (1×10^6/mL, 200 μL) and complete medium containing 10% FBS (600 μL). Transwell chambers were incubated in a 37 °C, 5% CO_2 incubator for 24 h. After discarding culture medium, the Transwell chambers were incubated with formaldehyde for fixation and 0.1% crystal violet for staining. The invasive cells in three randomly selected microscopic fields were photographed and the number of cell invasion was counted.

Fluorescence in Situ Hybridization (FISH) Assay

Hela cell slides were prepared and fixed in 4% paraformaldehyde (DEPC treatment) for 15 min. Cell slides were digested with 0.1% Triton X-100 (DEPC treatment) for 15 min and soaked in 2 × SSC solution (0.15 M NaCl and 0.015 M sodium citrate) at 37 °C for 30 min, dehydrated with gradient ethanol, and air dried. The hybridization buffer was incubated at 37 °C for 2 h. After denatured in 73 ± 1 °C water bath for 5 min, the FISH probe solution (1 μg/mL) was added into cell slides for hybridization at 37 °C overnight. After staining with DAPI, the fluorescence images were photographed using a laser scanning confocal microscope (Nikon Instruments Inc., Japan). The specific probe sequence utilized in the FISH assay for lncRNA H19 was: 5′-TTCATGTTGTGGGTTCTGGGAGCC-3′.

Dual-luciferase reporter assay

Hela cells at 70% confluence were seeded into a 96-well plate. For studying the targeting interaction between lncRNA H19 and miR-140, Hela cells were co-transfected with the dual-luciferase reporter vectors pmirGLO-lncRNA H19 wild-type (lncRNA H19 WT) or pmirGLO-lncRNA H19 mutated type (lncRNA H19 MUT) and miR-140 mimic or mimic NC using HighGene transfection reagent. For investigating the targeting interaction between miR-140 and ALDH1A1, Hela cells were co-transfected with the dual-luciferase reporter vectors pmirGLO-ALDH1A1 wild-type (ALDH1A1 WT) or pmirGLO-ALDH1A1 mutated type (ALDH1A1 MUT) and miR-140 mimic or mimic NC (Sangon Biotech, Shanghai, China). The luciferase activity was measured after 48 h of co-transfection using Pierce™ Cypridina-Firefly Luciferase Dual Assay Kit (Thermo Scientific).

Western blotting

Proteins in cells were extracted for western blotting as described previously [21]. Then the collected proteins were analyzed by SDS-PAGE and transferred to PVDF membrane (FFP24, Beyotime, China). Membranes were incubated with primary antibodies against ALDH1A1 (1:1000; #ab134188, Abcam, CB, UK), Bcl-2 (1:500; #ab196495, Abcam, CB, UK), Bax (1:1000, #ab32503, Abcam, CB, UK), and GAPDH (1:10,000; #ab181602, Abcam, CB, UK) at 4 °C overnight, followed by incubation with secondary antibody Goat Anti-Rabbit IgG H&L (HRP; 1:2000; #ab6721, Abcam, CB, UK). Protein band intensities were visualized utilizing an Electrochemical luminescence (ECL) reagents (P1000, APPLYGEN, Beijing, China).

Experiments with xenograft tumors

For the subcutaneous xenograft model, female BALB/c mice (4 weeks old) were purchased from HFK Bioscience Co. Ltd (Beijing, China). Then, sh-NC control and sh-H19-transduced Hela cells suspension at a density of 1×10^7 cells per mouse were subcutaneously injected into the dorsal side of mice ($n=4$ each group). Tumor size was measured every 3 days, and tumor volume was calculated according to the formula: volume $=0.5\times(\text{length}\times\text{width}^2)$. All mice were anesthetized with 200 mg/kg pentobarbital sodium and then sacrificed on day 18 after implantation, the resected xenograft tumor masses were harvested for subsequent weight and the analysis of qRT-PCR. All animal experiments were authorized by the Animal Ethics Committee of Yangzhou University (202405040). This study was conducted in accordance with the Animal Research: Reporting of In Vivo Experiments (ARRIVE) [22].

Statistical analysis

Statistical analyses were completed using GraphPad Prism (version 7.0; GraphPad Software, La Jolla, California). All data are presented as the means ± standard deviation. Unpaired *t* test was used to analyze differences between the two groups, and one-way ANOVA assay for multigroup analysis, followed by Tukey's post hoc test for comparison. The value of $P<0.05$ indicated significant results.

Results

LncRNA H19 expression was up-regulated in CC cells

To examine the potential role of lncRNA H19 as a key regulator in CC) development, we initially assessed the expression levels of lncRNA H19 in three distinct types of CC cells: Hela, Ca-Ski, and C33a cells. Our findings demonstrated a significant up-regulation of lncRNA H19 expression in the examined CC cells (Hela, Ca-Ski, and C33a) compared to normal cervical epithelial H8 cells ($P<0.01$, Fig. 1). Additionally, we observed that the expression of lncRNA H19 was significantly higher in Hela cells compared to Ca-Ski or C33a cells ($P<0.05$, Fig. 1). Based on these findings, we selected Hela cells for further functional experiments.

Downregulation of LncRNA H19 inhibited the malignant characteristics of CC cells

To explore the function of lncRNA H19 in CC, we suppressed lncRNA H19 expression in Hela and Ca-Ski cells by transfection with sh-H19. It was observed that lncRNA H19 expression was significantly suppressed after transfection (all $P<0.01$), confirming effective transfection (Figs. 2A and 3A). The results of CCK-8 assay revealed that Hela and Ca-Ski cells viability were evidently inhibited after suppression of lncRNA H19 (all $P<0.01$, Figs. 2B and 3B). Consistent results were obtained from colony formation assay that lncRNA H19 suppression dramatically reduced the proliferative capacities of Hela and Ca-Ski cells (all $P<0.01$, Figs. 2C and 3C). Moreover, by performing flow cytometry, we observed that lncRNA H19 suppression remarkably promoted Hela and Ca-Ski cells apoptosis (all $P<0.01$, Figs. 2D and 3D). Furthermore, scratch wound healing assay indicated that lncRNA H19 suppression effectively decreased the migratory abilities of Hela and Ca-Ski cells (all $P<0.01$, Figs. 2E and 3E). Similarly, Transwell assay showed that the invasive abilities of Hela and Ca-Ski

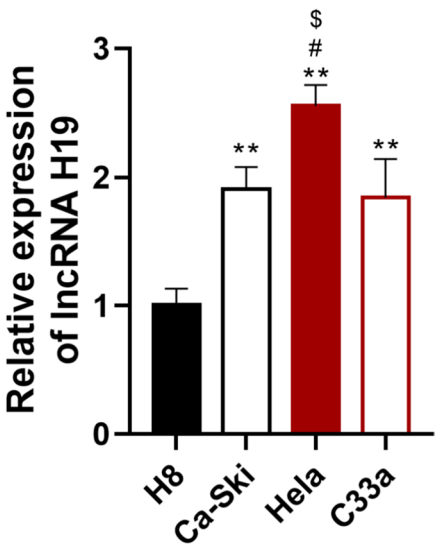

Fig. 1 The expression levels of lncRNA H19 were assessed in cervical cancer cells (Hela, Ca-Ski, and C33a) as well as normal cervical epithelial H8 cells. ** $P<0.01$ compared to H8 cells, $^{\#}$ $P<0.05$ compared to Ca-Ski cells, and $^{\$}$ $P<0.05$ compared to C33a cells

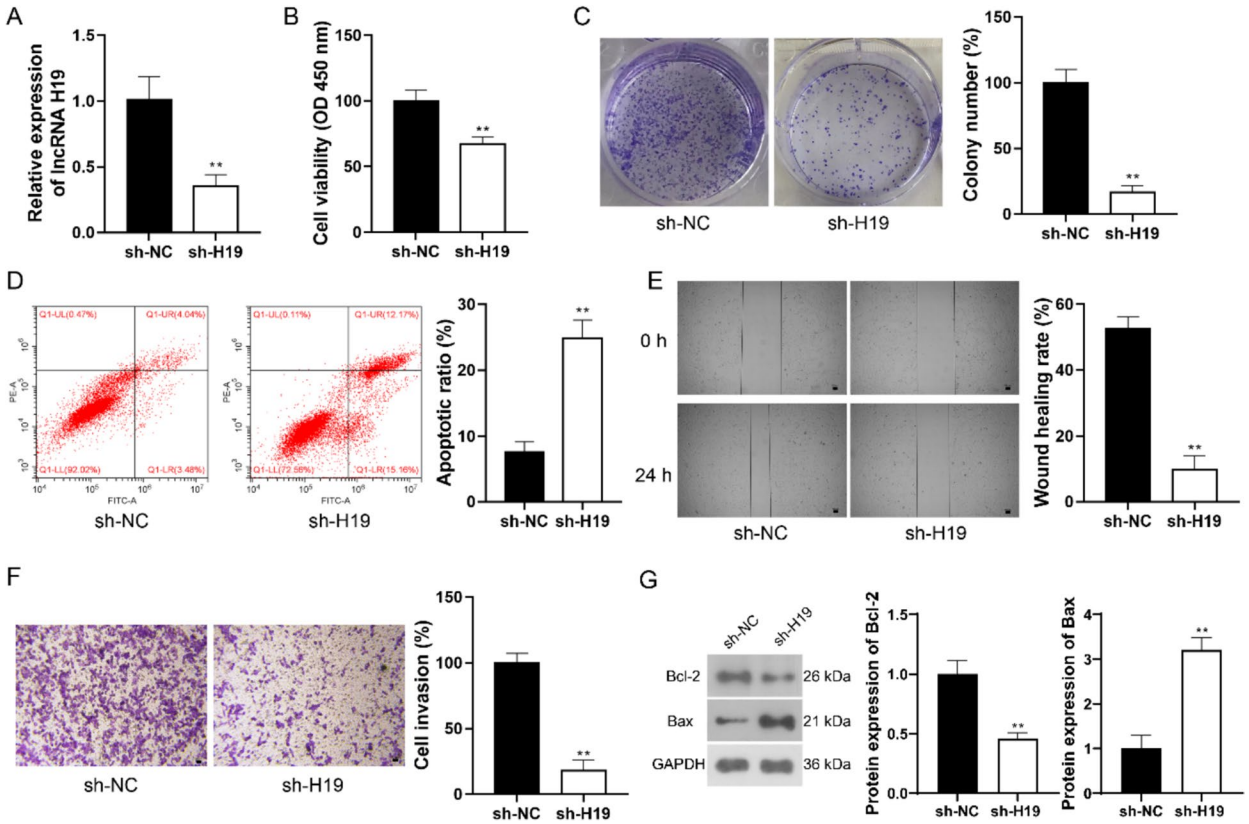

Fig. 2 The malignant biological properties of cervical cancer cells were inhibited upon suppression of lncRNA H19. Hela cells were transfected with either sh-H19 or sh-NC (negative control). **A** qRT-PCR analysis demonstrated the expression levels of lncRNA H19 in cells. **B** Cell viability of Hela cells was assessed using a CCK-8 assay (OD450 nm). **C** Colony formation assay was conducted to assess the proliferative capacities of Hela cells. **D** Flow cytometry analysis was performed to detect the level of apoptosis in Hela cells. **E** Scratch wound healing assay was conducted to evaluate the migratory abilities of Hela cells (scale bar: 50 μm). **F** Transwell assay was performed to determine the invasive abilities of Hela cells (scale bar: 50 μm). **G** Western blotting was employed to explore the expression levels of apoptosis related proteins Bcl-2 and Bax in Hela cells. ** $P < 0.01$ compared to the sh-NC group

cells were reduced after suppression of lncRNA H19 (all $P < 0.01$, Figs. 2F and 3F). Also, the expression levels of apoptosis related proteins Bcl-2 and Bax in Hela and Ca-Ski cells were both reversed after suppression of lncRNA H19 (all $P < 0.01$, Figs. 2G and 3G). These data strongly manifested that lncRNA H19 acted as an oncogene in CC.

LncRNA H19 was localized in the nucleus and exhibited targeting interactions with miR-140

To investigate the regulatory mechanism of lncRNA H19, we employed FISH assay to determine the cellular localization of lncRNA H19. Our results revealed that lncRNA H19 was primarily localized within the nucleus of cells (Fig. 4A). Bioinformatics analysis revealed that lncRNA H19 had the potential to bind miR-140 through starbase database (https://rnasysu.com/encori/) (Fig. 4B). Also, the dual-luciferase reporter assay was performed to further investigate the targeting interactions between lncRNA H19 and miR-140. Our results showed that miR-140 overexpression significantly inhibited the luciferase activity of lncRNA H19 WT construct ($P < 0.01$, Fig. 4C). In addition, we found that miR-140 was observably down-regulated in CC cells (Hela, Ca-Ski, and C33a cells) in relative to normal cervical epithelial H8 cells, especially Hela cells ($P < 0.01$, Fig. 4D). Moreover, suppression of lncRNA H19 resulted in a significant elevation in miR-140 expression ($P < 0.05$, Fig. 4E). These data indicated that lncRNA H19 exhibited targeting interactions with miR-140.

LncRNA H19 promoted the malignant biological properties of CC cells via targeting miR-140

To examine whether the promotion of CC development by lncRNA H19 is mediated through the modulation of miR-140, we proceeded by transfecting lncRNA H19-knockdown Hela cells with a miR-140 inhibitor. The results obtained from qRT-PCR analysis demonstrated

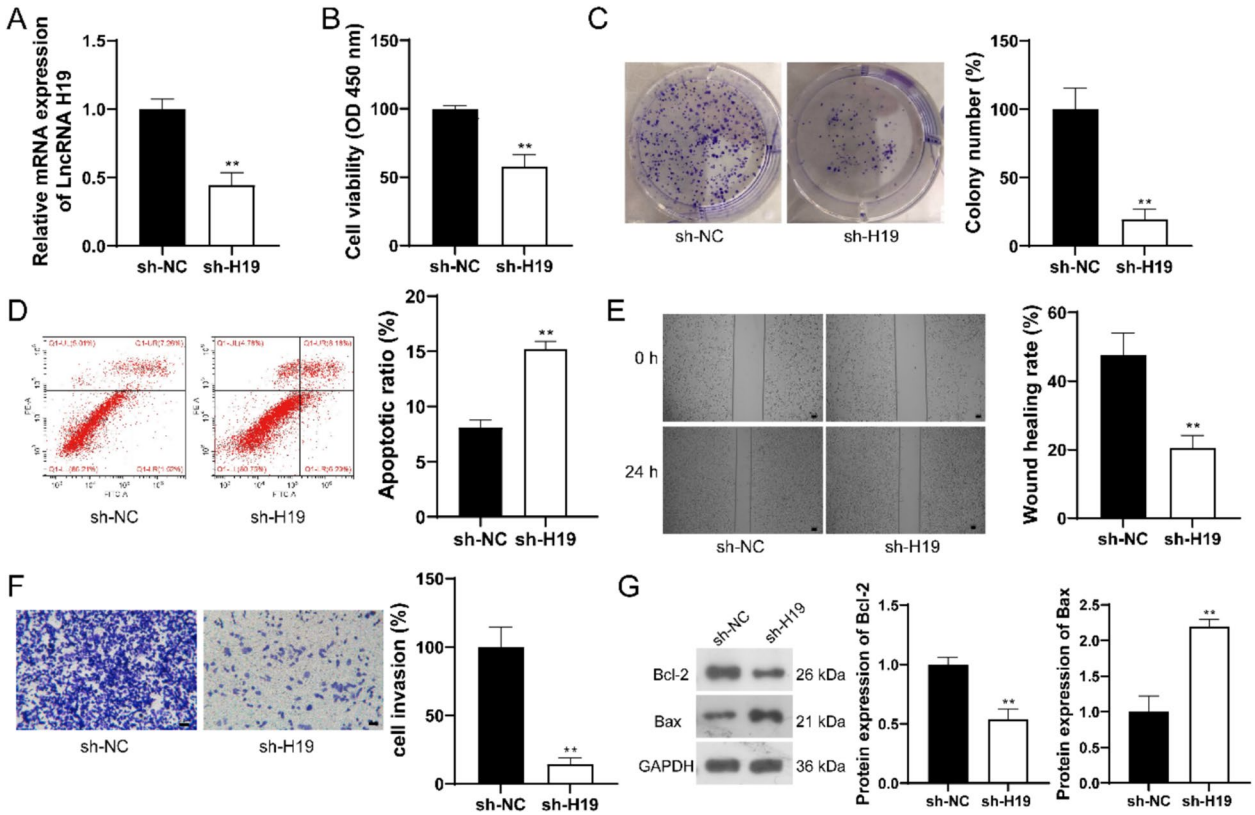

Fig. 3 The malignant biological properties of cervical cancer cells were inhibited upon suppression of lncRNA H19. Ca-Ski cells were transfected with either sh-H19 or sh-NC (negative control). **A** qRT-PCR analysis demonstrated the expression levels of lncRNA H19 in cells. **B** Cell viability of Ca-Ski cells was assessed using a CCK-8 assay (OD450 nm). **C** Colony formation assay was conducted to assess the proliferative capacities of Ca-Ski cells. **D** Flow cytometry analysis was performed to detect the level of apoptosis in Ca-Ski cells. **E** Scratch wound healing assay was conducted to evaluate the migratory abilities of Ca-Ski cells (scale bar: 50 μm). **F** Transwell assay was performed to determine the invasive abilities of Ca-Ski cells (scale bar: 50 μm). **G** Western blotting was employed to explore the expression levels of apoptosis related proteins Bcl-2 and Bax in Ca-Ski cells. ** $P < 0.01$ compared to the sh-NC group

that inhibition of miR-140 significantly reversed the impact of lncRNA H19 suppression on miR-140 expression ($P < 0.01$). However, no significant effect on lncRNA H19 expression was observed (Fig. 5A). In addition, the inhibition of miR-140 effectively reversed the effects of lncRNA H19 knockdown on the proliferation, apoptosis, migration, and invasion of Hela cells ($P < 0.05$, Fig. 5B–G). All data suggested that LncRNA H19 promoted the malignant biological properties of CC cells via targeting miR-140.

LncRNA H19 regulated ALDH1A1 expression via sponging miR-140

To explore the downstream mechanism of lncRNA H19/miR-140 axis, the binding sites of ALDH1A1 and miR-140 were explored through mirwalk database (http://mirwalk.umm.uni-heidelberg.de/) (Fig. 6A). Also, the targeting relationship between miR-140 and ALDH1A1 using dual-luciferase reporter assay was explored. As a result, miR-140 overexpression visibly inhibited the luciferase activity of ALDH1A1 WT ($P < 0.01$), but had no significant effect on the luciferase activity of ALDH1A1 MUT, confirming the targeting interactions between miR-140 and ALDH1A1 (Fig. 6B). Moreover, ALDH1A1 was observably up-regulated in CC cells (Hela, Ca-Ski, and C33a cells) compared to that in H8 cells (all $P < 0.01$, Fig. 6C and E). Furthermore, we observed a significant reduction in ALDH1A1 expression following the suppression of lncRNA H19. However, this reduction was notably reversed upon inhibition of miR-140 (all $P < 0.01$, Figs. 6D and F). These data indicated that lncRNA H19 regulated ALDH1A1 expression via sponging miR-140.

Inhibition of lncRNA H19 diminishes tumor growth in vivo

To evaluate whether lncRNA H19 expression is required for tumor growth in vivo, sh-H19-infected or sh-NC-transduced Hela cells were implanted into mice by subcutaneous injection. Xenograft tumors derived from sh-H19-infected Hela cells exhibited suppressed growth compared with the sh-NC group (Fig. 7A–C). Moreover,

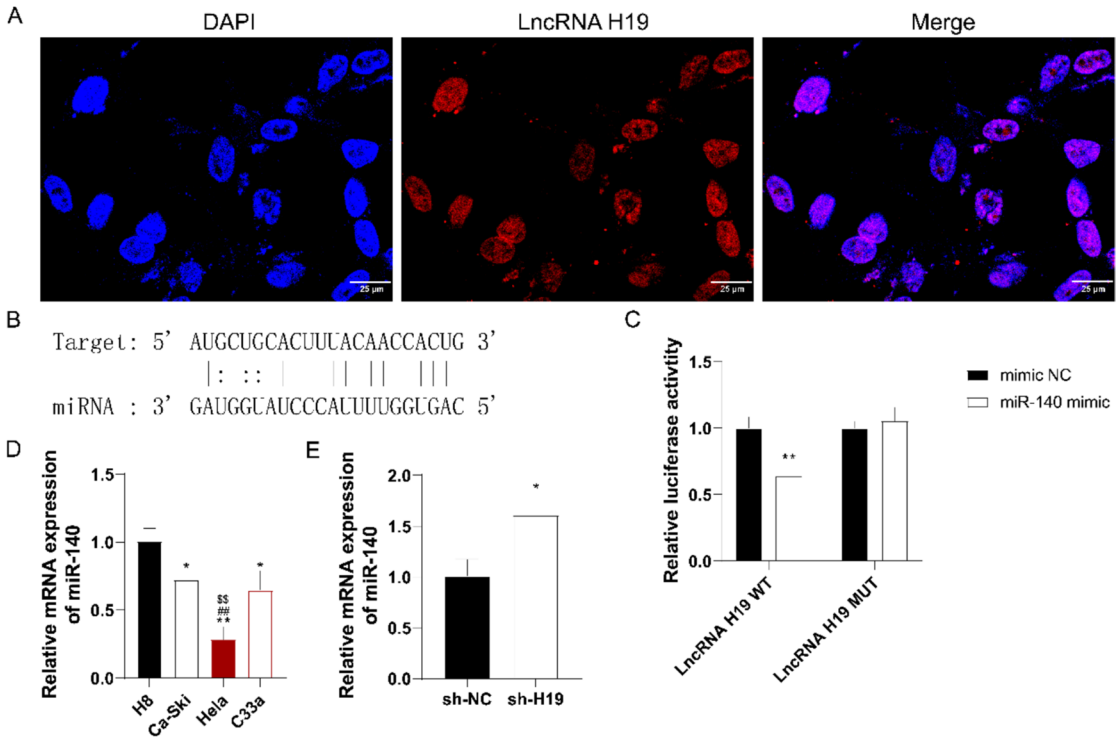

Fig. 4 The localization of lncRNA H19 within cells and its interactions with miR-140 were investigated. **A** Fluorescence in situ hybridization (FISH) assay was employed to visualize the localization of lncRNA H19 (scale bar: 25 μm). **B** The binding sites of lncRNA H19 and miR-140 through starbase database. **C** Dual-luciferase reporter assay demonstrated the targeting interactions between lncRNA H19 and miR-140. $^{**}P<0.01$ compared to the mimic NC group. **D** The expression of miR-140 was measured in cervical cancer cells (Hela, Ca-Ski, and C33a) and normal cervical epithelial H8 cells. $^{*}P<0.05$, $^{**}P<0.01$ compared to H8 cells, $^{\#\#}P<0.01$ compared to Ca-Ski cells, and $^{\$\$}P<0.01$ compared to C33a cells. **E** The expression of miR-140 was evaluated in Hela cells transfected with either sh-H19 or sh-NC. $^{*}P<0.05$ compared to the sh-NC group

(See figure on next page.)

Fig. 5 Downregulation of miR-140 reversed the inhibitory effects of lncRNA H19 suppression on the malignant biological properties of cervical cancer cells. LncRNA H19-knockdown Hela cells were transfected with a miR-140 inhibitor. **A** qRT-PCR analysis was conducted to assess the expression levels of lncRNA H19 and miR-140 in cells. **B** Cell viability of Hela cells was evaluated using a CCK-8 assay (OD450 nm). **C** Colony formation assay was conducted to assess the proliferative capacities of Hela cells. **D** Flow cytometry analysis was performed to detect the level of apoptosis in Hela cells. **E** Scratch wound healing assay was conducted to evaluate the migratory abilities of Hela cells (scale bar: 50 μm). **F** Transwell assay was performed to determine the invasive abilities of Hela cells (scale bar: 50 μm). **G** Western blotting was employed to explore the expression levels of apoptosis related proteins Bcl-2 and Bax in Hela cells. $^{**}P<0.01$ compared to the vector group, $^{\#}P<0.05$ and $^{\#\#}P<0.01$ compared to the sh-H19 + inhibitor NC group

in sh-H19-infected Hela cells group, lncRNA H19 and ALDH1A1 levels were under-expressed and miR-140 expression was elevated (Figs. 7D and E). All these results also suggested that reduction of lncRNA H19 diminishes tumor growth via targeting the miR-140/ALDH1A1 axis.

Discussion

CC is a main cancer worldwide with a high incidence. The discovery of novel biomarker can profoundly impact the early diagnosis, disease surveillance, and treatment of many cancers including CC [23]. Our study demonstrated that lncRNA H19 was up-regulated in CC cells and its suppression inhibited the malignant properties of CC cells. LncRNA H19 was localized in the nucleus and targeted miR-140. Furthermore, miR-140 downregulation reversed the inhibitory effects of lncRNA H19 suppression on CC cell malignancy. Additionally, miR-140 targeted and regulated the expression of ALDH1A1. These findings suggest that lncRNA H19 promotes CC development by functioning as a ceRNA for miR-140 and modulating ALDH1A1 expression.

LncRNAs have gained massive attention due to their significant roles in modulating diverse physiological and pathological processes [24, 25]. LncRNAs can exert

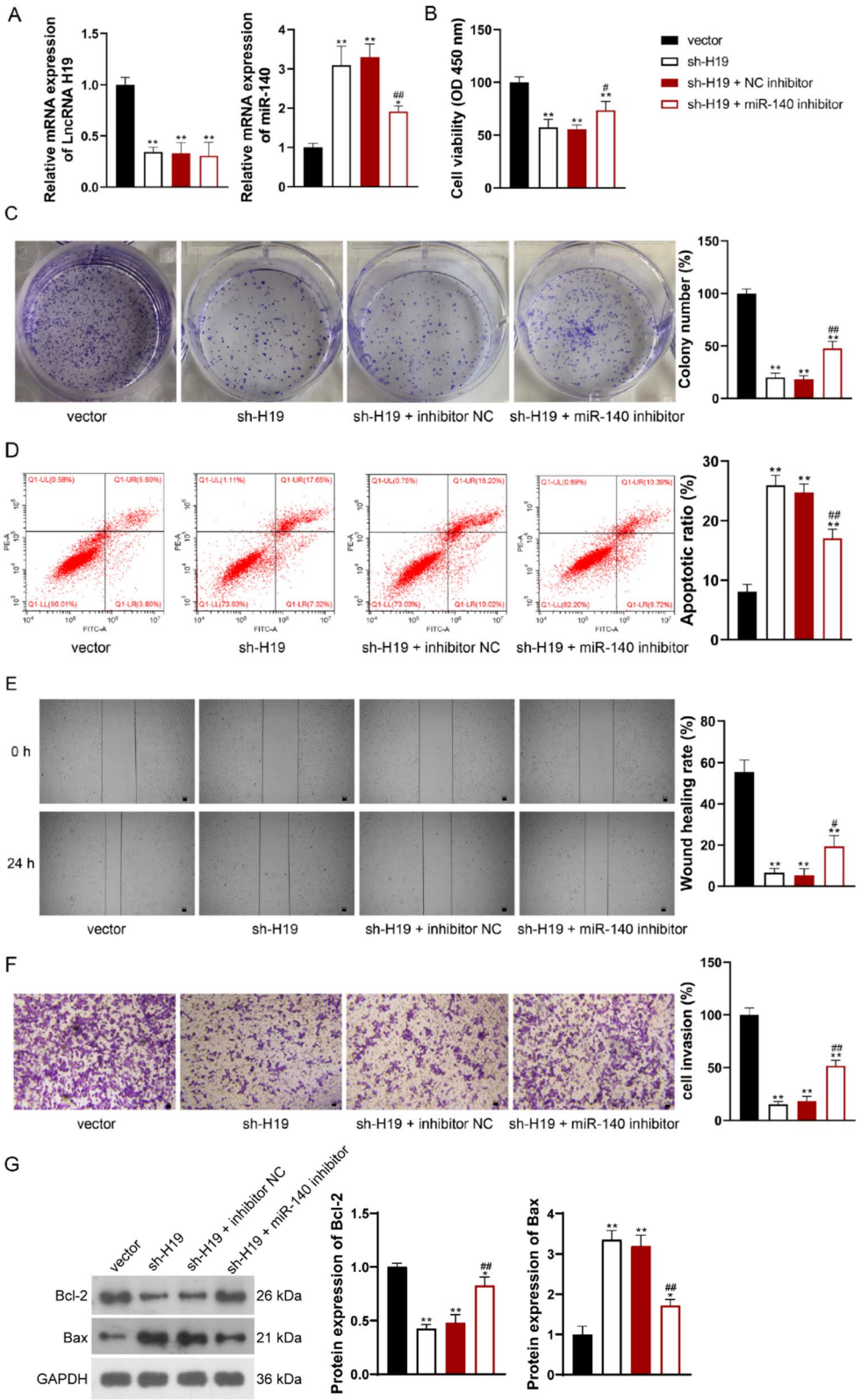

Fig. 5 (See legend on previous page.)

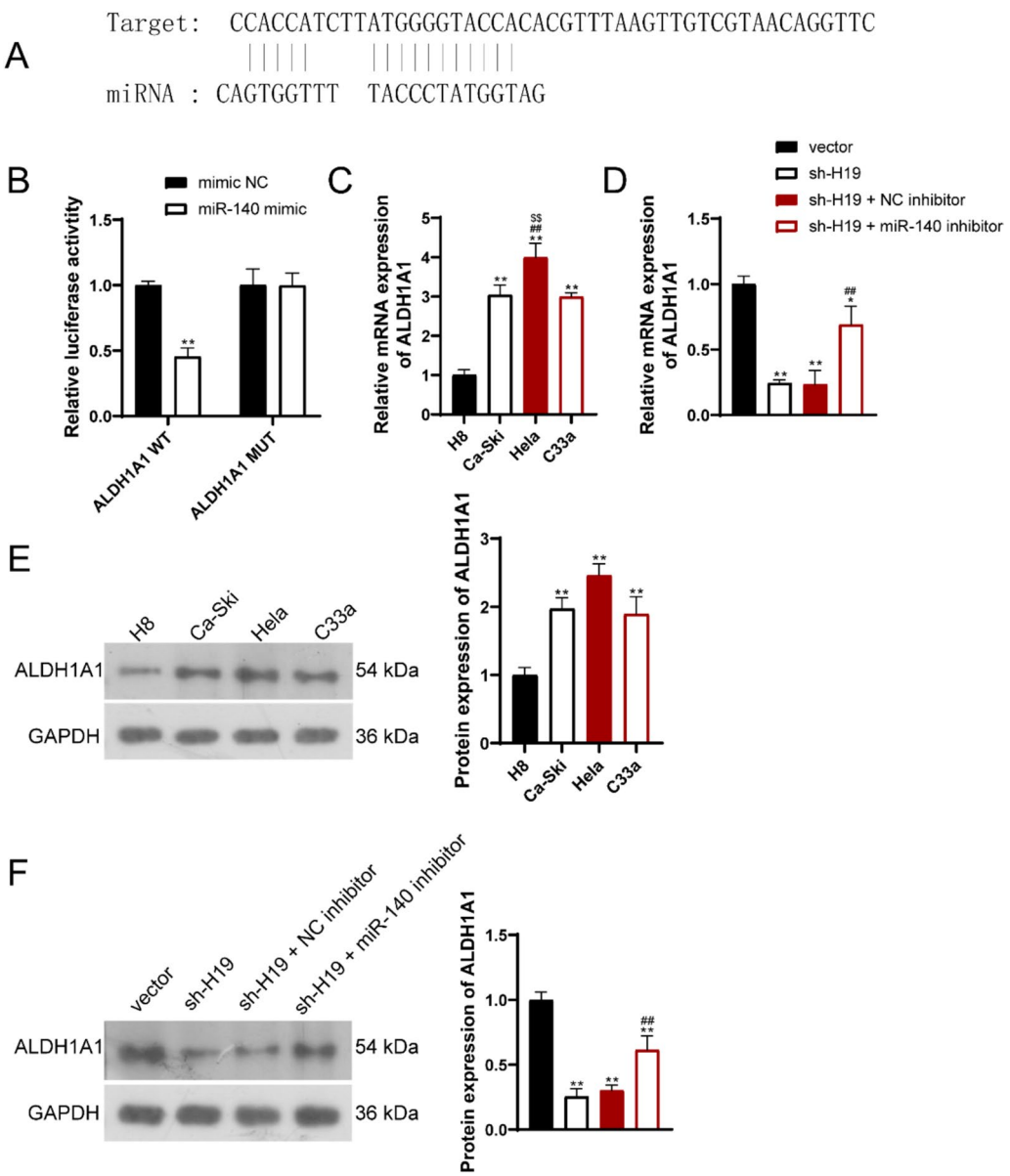

Fig. 6 LncRNA H19 targeted miR-140/ALDH1A1 axis in cervical cancer cells. **A** The binding sites of ALDH1A1 and miR-140 through mirwalk database. **B** Dual-luciferase reporter assay was performed to demonstrate the targeting interactions between ALDH1A1 and miR-140. $^{**}P < 0.01$ compared to the mimic NC group. **C** The mRNA expression levels of ALDH1A1 were examined in cervical cancer cells (Hela, Ca-Ski, and C33a) and normal cervical epithelial H8 cells. $^{**}P < 0.01$ compared to H8 cells, $^{\#\#}P < 0.01$ compared to Ca-Ski cells, and $^{\$\$}P < 0.01$ compared to C33a cells. **D** The mRNA expression levels of ALDH1A1 were analyzed. **E** The protein expression level of ALDH1A1 was examined in cervical cancer cells (Hela, Ca-Ski, and C33a) and normal cervical epithelial H8 cells. $^{**}P < 0.01$ compared to H8 cells. **F** Western blotting was employed to explore the protein expression levels of ALDH1A1. $^{**}P < 0.01$ compared to the vector group, $^{\#\#}P < 0.01$ compared to the sh-H19 + inhibitor NC group

oncogenic or tumor suppressor roles in human cancers, including CC [26, 27]. Accumulating evidence has indicated that lncRNA H19 functions as an oncogene in various cancers [28, 29]. It has been reported that lncRNA H19 accelerates cell proliferation, invasion, and migration in ovarian cancer [30]. Elevated lncRNA H19 expression is related to colon cancer recurrence [31]. In CC, lncRNA H19 has the biological role in promoting cell migration and proliferation [32]. Consistent with these findings, the expression of lncRNA H19 was found to be up-regulated in CC cells. Moreover, the suppression of lncRNA H19 led to a substantial reduction in cell proliferation, migration, and invasion in CC cells, and remarkably promoted CC cell apoptosis. Based on these observations, we can

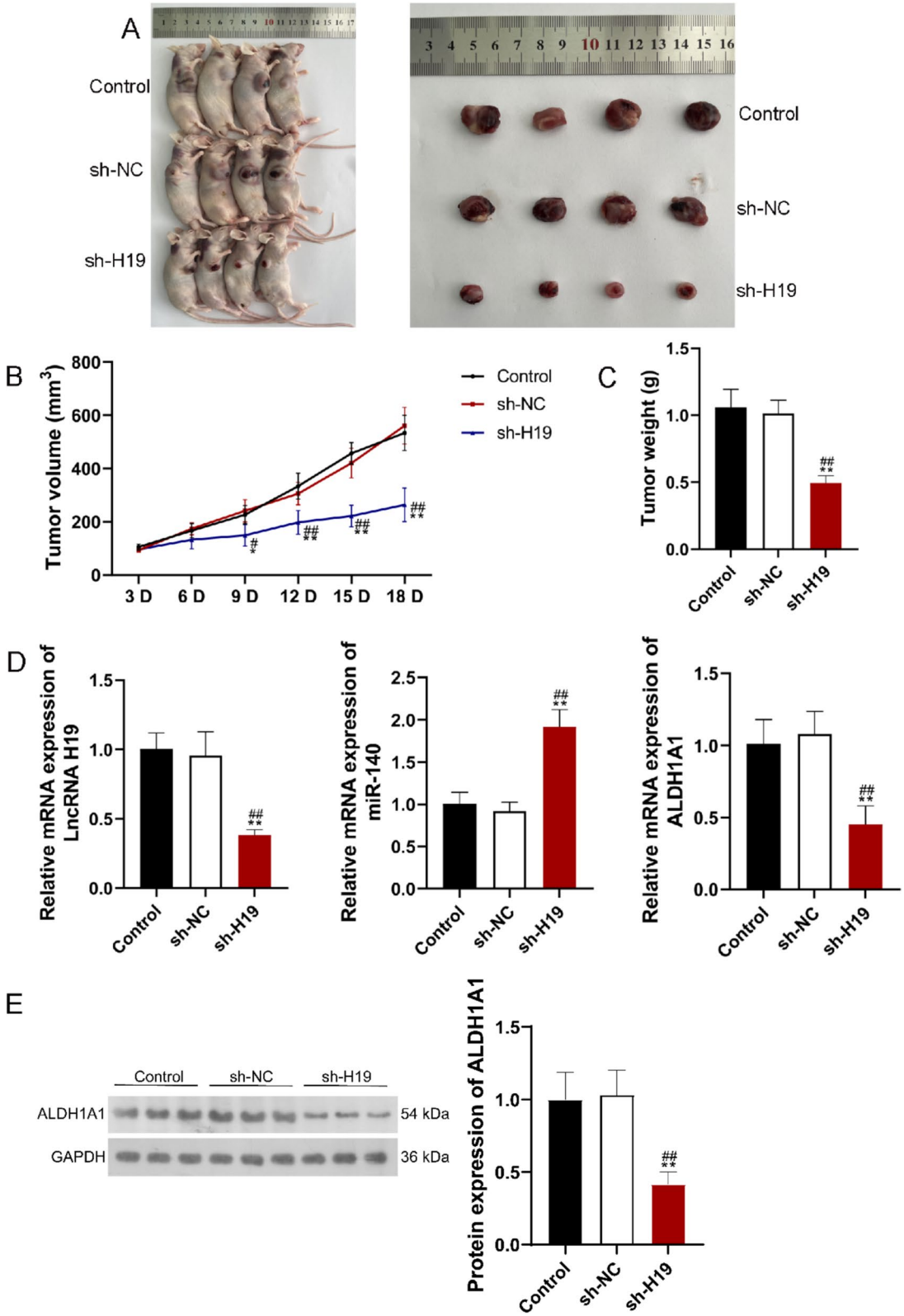

Fig. 7 LncRNA H19 inhibition hinders tumor growth in vivo. **A** Representative images of xenograft tumors isolated from nude mice in the different groups. **B** Growth curve of the xenograft tumors. **C** Weight of the xenograft tumors. **D** qRT-PCR for lncRNA H19, miR-140 and ALDH1A1 mRNA in the xenograft tumors. 3 biological replicates for each group, and 4 mice in each group. **E** Western blotting was employed to explore the expression levels of ALDH1A1. $^{*}P<0.05$, $^{**}P<0.01$ compared to the Control group, $^{\#}P<0.05$, $^{\#\#}P<0.01$ compared to the sh-NC group

conclude that lncRNA H19 plays an oncogenic role in the context of CC. According to these conclusions, lncRNA H19 could serve as a useful diagnostic tool and lncRNA H19 treatment target for CC.

It was widely known that lncRNAs can act as ceRNAs for miRNAs, thus modulating tumor progression in CC [33, 34]. Dysregulation of miRNAs contributes to tumorigenesis and progression of many human cancers [35–37]. Numerous studies have also revealed that miRNAs affect the pathophysiologic process of CC [38, 39]. This study analyzed miR-140 expression in CC cells and investigated the relationship between lncRNA H19 and miR-140. Growing studies have reported that miR-140 participates in multiple cell biological functions and affects the pathogenesis of diverse cancers [40], such as esophageal cancer [41] and thyroid cancer [42]. Chang et al. revealed that lncRNA PVT1 accelerated CC development by sponging miR-140-5p to enhance Smad3 expression [43]. Consistent with previous findings [14, 15], we also found that miR-140 was down-regulated in CC tumor cells, and lncRNA H19 could sponge miR-140. Moreover, inhibition of miR-140 significantly reversed the inhibitory effect of lncRNA H19 suppression on the malignant biological properties of CC cells. Overall, it can be concluded that lncRNA H19 may promote CC development via sponging miR-140. Thus, our results provide a basis for future efforts to develop novel therapeutic strategies for CC.

Furthermore, we confirmed that miR-140 could directly target ALDH1A1. The ALDH family consists of 19 different isoforms, and the ALDH activity is a marker of cancer stem-like cells [44]. Increased ALDH1 expression was observed in cervical tumors and was related to poor prognosis and chemotherapy resistance in CC patients [45, 46]. Among the six ALDH1 isoenzymes, ALDH1A1 is considered as a main contributor of ALDH1 activity, which shows vital pathophysiological functions in various cancers [47]. It has been observed that ALDH1A1 is implicated in CC precancerous process and may serve as early diagnostic marker for CC [19]. Here, we found that ALDH1A1 was up-regulated in CC cells. Also, suppression of lncRNA H19 caused the decrease of ALDH1A1 expression, which was reversed after inhibition of miR-140. Based on our findings, we postulate that ALDH1A1 could potentially contribute to the development of CC. Furthermore, we propose that lncRNA H19 may promote the expression of ALDH1A1 by acting as a sponge for miR-140, thereby sequestering miR-140 and relieving its inhibitory effects on ALDH1A1.

Our study still has some limitations. First, the lncRNA H19, miR-140, and ALDH1A1 expression was not confirmed in clinical cervical tumors. Second, the role and regulatory mechanism of lncRNA H19, miR-140, and ALDH1A1 was not investigated in protein level. Third, independent biological replicates should be conducted in this study. In addition, the US-FDA has approved some siRNA delivery systems for treating various diseases [48–50], whether nanoparticle loading siRNA could be used for clinical therapy of CC need further explore. Lastly, correlation between drug resistance and the activation of H19/miR-140/ALDH1A1 axis should be further analyzed. More studies are warranted to explore their clinical application as potential biomarkers or treatment targets.

Conclusion

In summary, our results reveal that lncRNA H19 promotes carcinogenesis of CC and elevates ALDH1A1 expression through functioning as a ceRNA of miR-140. Detecting or targeting lncRNA H19, miR-140, and ALDH1A1 expression may aid for CC diagnosis and treatment. Overall, our study provides new insights into the pathogenesis of CC and offers potential avenues for the development of novel therapeutic strategies.

Abbreviations

ALDH1	Aldehyde dehydrogenase 1
CC	Cervical cancer
ceRNAs	Competing endogenous RNAs
FISH	Fluorescence in situ hybridization
lncRNA H19	Long non-coding RNA H19
miRNAs	MicroRNAs
MOI	Multiplicity of infection
ncRNAs	Non-coding RNAs
OS	Overall survival
qRT-PCR	Quantitative reverse transcriptase polymerase chain reaction

Acknowledgements

Not applicable.

Author contributions

J. M.: Drafting the manuscript; F. C.: Revision of manuscript for important intellectual content; Y. F.: Analysis and interpretation of data; M. Z.: Analysis and interpretation of data; Q. R.: Statistical analysis; K. L.: Acquisition of data; Z. N.: Carried out experimental; S. X.: Statistical analysis; L. T.: Reviewed the manuscript; A. A.: Carried out experimental; L. Y.: Conception and design of the research, Obtaining funding. All authors read and approved the final manuscript.

Funding

This research was funded by General project of the Natural Science Foundation of Xinjiang UygurAutonomous Region (grant number 2022D01A01).

Availability of data and materials

No datasets were generated or analysed during the current study.

Declarations

Ethics approval and consent to participate

All animal experiments were authorized by the Animal Ethics Committee of Yangzhou University (202405040).

Competing interests

The authors declare no competing interests.

Received: 7 November 2024 Accepted: 31 January 2025
Published online: 12 February 2025

References

1. Li M, Yang Z-L, Chen Z-Y, Jiang L, Hong S-Y. Cervical cancer screening and prevention. Cancer Screen Prev. 2023;2(1):42–50. https://doi.org/10.14218/csp.2022.00009.
2. Nisha P, Srushti P, Palak KP. Comprehensive review on analytical and bioanalytical methods for quantification of anti-angiogenic agents used in treatment of cervical cancer. Curr Pharm Anal. 2023;19(10):735–44.
3. Arbyn M, Weiderpass E, Bruni L, de Sanjose S, Saraiya M, Ferlay J, et al. Estimates of incidence and mortality of cervical cancer in 2018: a worldwide analysis. Lancet Glob Health. 2020;8(2):e191–203. https://doi.org/10.1016/S2214-109X(19)30482-6PMC7025157.
4. Kagabu M, Nagasawa T, Sato C, Fukagawa Y, Kawamura H, Tomabechi H, et al. Immunotherapy for uterine cervical cancer using checkpoint inhibitors: future directions. Int J Mol Sci. 2020;21(7):2335. https://doi.org/10.3390/ijms21072335PMC7177858.
5. Small W Jr, Bacon MA, Bajaj A, Chuang LT, Fisher BJ, Harkenrider MM, et al. Cervical cancer: A global health crisis. Cancer. 2017;123(13):2404–12. https://doi.org/10.1002/cncr.30667.
6. Kim VN. MicroRNA biogenesis: coordinated cropping and dicing. Nat Rev Mol Cell Biol. 2005;6(5):376–85. https://doi.org/10.1038/nrm1644.
7. Dai T, Li J, Ye L, Yu H, Deng M, Liu W, et al. Prognostic Role and potential mechanisms of N6-methyladenosine-related long noncoding RNAs in hepatocellular carcinoma. J Clin Transl Hepatol. 2022;10(2):308–20. https://doi.org/10.14218/jcth.2021.00096.
8. Li P, Ma X, Gu X. LncRNA MAFG-AS1 is involved in human cancer progression. Eur J Med Res. 2023;28(1):497. https://doi.org/10.1186/s40001-023-01486-9PMC10631199.
9. Liu H, Zhang L, Ding X, Sui X. LINC00861 inhibits the progression of cervical cancer cells by functioning as a ceRNA for miR-513b-5p and regulating the PTEN/AKT/mTOR signaling pathway. Mol Med Rep. 2021;23(1):1–1. https://doi.org/10.3892/mmr.2020.11662.
10. Luo L, Wang M, Li X, Luo C, Tan S, Yin S, et al. A novel mechanism by which ACTA2-AS1 promotes cervical cancer progression: acting as a ceRNA of miR-143-3p to regulate SMAD3 expression. Cancer Cell Int. 2020;20(1):1–13. https://doi.org/10.1186/s12935-020-01471-w.
11. Yang J, Qi M, Fei X, Wang X, Wang K. LncRNA H19: a novel oncogene in multiple cancers. Int J Biol Sci. 2021;17(12):3188–208. https://doi.org/10.7150/ijbs.62573PMC8375239.
12. Iempridee T. Long non-coding RNA H19 enhances cell proliferation and anchorage-independent growth of cervical cancer cell lines. Exp Biol Med (Maywood). 2017;242(2):184–93. https://doi.org/10.1177/1535370216670542PMC5167123.
13. Roychowdhury A, Samadder S, Das P, Mazumder DI, Chatterjee A, Addya S, et al. Deregulation of H19 is associated with cervical carcinoma. Genomics. 2020;112(1):961–70. https://doi.org/10.1016/j.ygeno.2019.06.012.
14. Song D, Zhao M, Feng L, Wang P, Li Y, Li W. Salidroside attenuates acute lung injury via inhibition of inflammatory cytokine production. Biomed Pharmacother. 2021;142: 111949. https://doi.org/10.1016/j.biopha.2021.111949.
15. Zhao H, Peng R, Liu Q, Liu D, Du P, Yuan J, et al. The lncRNA H19 interacts with miR-140 to modulate glioma growth by targeting iASPP. Arch Biochem Biophys. 2016;610:1–7. https://doi.org/10.1016/j.abb.2016.09.014.
16. Guo Y, Luo S. miR-140-5p inhibits cervical cancer cell phenotypes via downregulating FEN1 to halt the cell cycle. Mol Med Rep. 2020;22(6):4919–30. https://doi.org/10.3892/mmr.2020.11552.
17. Li Q, Yao Y, Eades G, Liu Z, Zhang Y, Zhou Q. Downregulation of miR-140 promotes cancer stem cell formation in basal-like early stage breast cancer. Oncogene. 2014;33(20):2589–600. https://doi.org/10.1038/onc.2013.226PMC3883868.
18. Zhang L, Dong B, Yuan X. Expression of ALDH1 plays the important role during generation and progression in human cervical cancer. Biotechnol Genet Eng Rev. 2023. https://doi.org/10.1080/02648725.2022.2161211.
19. Tulake W, Yuemaier R, Sheng L, Ru M, Lidifu D, Abudula A. Upregulation of stem cell markers ALDH1A1 and OCT4 as potential biomarkers for the early detection of cervical carcinoma. Oncol Lett. 2018;16(5):5525–34. https://doi.org/10.3892/ol.2018.9381.
20. Singaravelan S, Sivaperuman A, Calambur NN. A review on PCR and POC-PCR—a boon in the diagnosis of COVID-19. Curr Pharm Anal. 2022;18(8):745–64. https://doi.org/10.2174/1573412918666220509032754.
21. Yang R, Gao W, Wang Z, Jian H, Peng L, Yu X, et al. Polyphyllin I induced ferroptosis to suppress the progression of hepatocellular carcinoma through activation of the mitochondrial dysfunction via Nrf2/HO-1/GPX4 axis. Phytomed Int J Phytother Phytopharmacol. 2024;122: 155135. https://doi.org/10.1016/j.phymed.2023.155135.
22. Kilkenny C, Browne WJ, Cuthill IC, Emerson M, Altman DG. Improving bioscience research reporting: the ARRIVE guidelines for reporting animal research. PLoS Biol. 2010;8(6): e1000412. https://doi.org/10.1371/journal.pbio.1000412PMC2893951.
23. Dasari S, Wudayagiri R, Valluru L. Cervical cancer: biomarkers for diagnosis and treatment. Clin Chim Acta. 2015;445:7–11. https://doi.org/10.1016/j.cca.2015.03.005.
24. Zhao X, Wang Y, Xia H, Liu S, Huang Z, He R, et al. Roles and molecular mechanisms of biomarkers in hepatocellular carcinoma with microvascular invasion: a review. J Clin Transl Hepatol. 2023;11(5):1170–83. https://doi.org/10.14218/jcth.2022.00013s.
25. Huang L, Xiong S, Liu H, Li M, Zhang R, Liu Y, et al. Bioinformatics analysis of the inflammation-associated lncRNA-mRNA coexpression network in type 2 diabetes. J Renin-Angiotensin-Aldosterone Syst JRAAS. 2023;2023:6072438. https://doi.org/10.1155/2023/6072438 PMC9977555 commercial, or academic conflicts of interest, and they have nothing to disclose.
26. Zhou M, Liu L, Wang J, Liu W. The role of long noncoding RNAs in therapeutic resistance in cervical cancer. Front Cell Dev Biol. 2022;10:1060909. https://doi.org/10.3389/fcell.2022.1060909.
27. He J, Huang B, Zhang K, Liu M, Xu T. Long non-coding RNA in cervical cancer: From biology to therapeutic opportunity. Biomed Pharmacother. 2020;127: 110209. https://doi.org/10.1016/j.biopha.2020.110209.
28. Hashemi M, Moosavi MS, Abed HM, Dehghani M, Aalipour M, Heydari EA, et al. Long non-coding RNA (lncRNA) H19 in human cancer: from proliferation and metastasis to therapy. Pharmacol Res. 2022;184: 106418. https://doi.org/10.1016/j.phrs.2022.106418.
29. Yoshimura H, Matsuda Y, Yamamoto M, Kamiya S, Ishiwata T. Expression and role of long non-coding RNA H19 in carcinogenesis. Front Biosci (Landmark Ed). 2018;23(4):614–25. https://doi.org/10.2741/4608.
30. Xu H, Ding Y, Yang X. Overexpression of long noncoding RNA H19 downregulates miR-140–5p and activates PI3K/AKT signaling pathway to promote invasion, migration and epithelial-mesenchymal transition of ovarian cancer cells. Biomed Res Int. 2021;2021:6619730. https://doi.org/10.1155/2021/6619730.
31. O'Brien SJ, Scheurlen K, Rochet A, Fiechter C, Paas M, Pan J, et al. Increased expression of long non-coding RNA H19 is associated with colon cancer recurrence. J Surg Res. 2022;269:59–68. https://doi.org/10.1016/j.jss.2021.08.004.
32. Cáceres-Durán MÁ, Ribeiro-dos-Santos Â, Vidal AF. Roles and mechanisms of the long noncoding RNAs in cervical cancer. Int J Mol Sci. 2020;21(24):9742. https://doi.org/10.3390/ijms21249742.
33. Li Y, Wang H, Huang H. Long non-coding RNA MIR205HG function as a ceRNA to accelerate tumor growth and progression via sponging miR-122–5p in cervical cancer. Biochem Biophys Res Commun. 2019;514(1):78–85. https://doi.org/10.1016/j.bbrc.2019.04.102.
34. Han Q, Wu W, Cui Y. LINC00337 regulates KLF5 and maintains stem-cell like traits of cervical cancer cells by modulating miR-145. Front Oncol. 2020;10:1433. https://doi.org/10.3389/fonc.2020.01433.
35. Doghish AS, Ismail A, El-Mahdy HA, Elkady MA, Elrebehy MA, Sallam AM. A review of the biological role of miRNAs in prostate cancer suppression and progression. Int J Biol Macromol. 2022;197:141–56. https://doi.org/10.1016/j.ijbiomac.2021.12.141.
36. Smolarz B, Durczynski A, Romanowicz H, Szyllo K, Hogendorf P. miRNAs in cancer (review of literature). Int J Mol Sci. 2022;23(5):2805. https://doi.org/10.3390/ijms23052805.
37. Fathi D, Elballal MS, Elesawy AE, Abulsoud AI, Elshafei A, Elsakka EGE, et al. An emphasis on the interaction of signaling pathways highlights the role of miRNAs in the etiology and treatment resistance of gastric cancer. Life Sci. 2023;322: 121667. https://doi.org/10.1016/j.lfs.2023.121667.

38. Doghish AS, Ali MA, Elyan SS, Elrebehy MA, Mohamed HH, Mansour RM, et al. miRNAs role in cervical cancer pathogenesis and targeted therapy: Signaling pathways interplay. Pathol Res Pract. 2023;244: 154386. https://doi.org/10.1016/j.prp.2023.154386.
39. Mitra T, Elangovan S. Cervical cancer development, chemoresistance, and therapy: a snapshot of involvement of microRNA. Mol Cell Biochem. 2021;476(12):4363–85. https://doi.org/10.1007/s11010-021-04249-4.
40. Taheri F, Ebrahimi SO, Heidari R, Pour SN, Reiisi S. Mechanism and function of miR-140 in human cancers: a review and in silico study. Pathol Res Pract. 2023;241: 154265. https://doi.org/10.1016/j.prp.2022.154265.
41. Yang S, Li X, Shen W, Hu H, Li C, Han G. MicroRNA-140 represses esophageal cancer progression via targeting ZEB2 to regulate Wnt/β-catenin pathway. J Surg Res. 2021;257:267–77. https://doi.org/10.1016/j.jss.2020.07.074.
42. Yu Q, Sun W, Hua H, Chi Y, Liu X, Dong A, et al. Downregulation of miR-140 is correlated with poor prognosis and progression of thyroid cancer. Endocr Metab Immune Disord Drug Targets (Formerly Current Drug Targets-Immune, Endocrine & Metabolic Disorders). 2021;21(4):749–55. https://doi.org/10.2174/1871530320666200724180742.
43. Chang Q-Q, Chen C-Y, Chen Z, Chang S. LncRNA PVT1 promotes proliferation and invasion through enhancing Smad3 expression by sponging miR-140-5p in cervical cancer. Radiol Oncol. 2019;53(4):443–52. https://doi.org/10.2478/raon-2019-0048.
44. Huddle BC, Grimley E, Buchman CD, Chtcherbinine M, Debnath B, Mehta P, et al. Structure-based optimization of a novel class of aldehyde dehydrogenase 1A (ALDH1A) subfamily-selective inhibitors as potential adjuncts to ovarian cancer chemotherapy. J Med Chem. 2018;61(19):8754–73. https://doi.org/10.1021/acs.jmedchem.8b00930.
45. Yao T, Wu Z, Liu Y, Rao Q, Lin Z. Aldehyde dehydrogenase 1 (ALDH1) positivity correlates with poor prognosis in cervical cancer. J Int Med Res. 2014;42(4):1038–42. https://doi.org/10.1177/0300060514527060.
46. Xie Q, Liang J, Rao Q, Xie X, Li R, Liu Y, et al. Aldehyde dehydrogenase 1 expression predicts chemoresistance and poor clinical outcomes in patients with locally advanced cervical cancer treated with neoadjuvant chemotherapy prior to radical hysterectomy. Ann Surg Oncol. 2016;23(1):163–70. https://doi.org/10.1245/s10434-015-4555-7.
47. Yue H, Hu Z, Hu R, Guo Z, Zheng Y, Wang Y, et al. ALDH1A1 in cancers: bidirectional function, drug resistance, and regulatory mechanism. Front Oncol. 2022;12: 918778. https://doi.org/10.3389/fonc.2022.918778.
48. Wang K, Chen H, Qin S, Chen S, Zhang Q, Chen J, et al. Co-delivery of pirfenidone and siRNA in ZIF-based nanoparticles for dual inhibition of hepatic stellate cell activation in liver fibrotic therapy. Colloids Surf B Biointerfaces. 2023;231: 113567. https://doi.org/10.1016/j.colsurfb.2023.113567.
49. Chen Y, Huang Y, Li Q, Luo Z, Zhang Z, Huang H, et al. Targeting Xkr8 via nanoparticle-mediated in situ co-delivery of siRNA and chemotherapy drugs for cancer immunochemotherapy. Nat Nanotechnol. 2023;18(2):193–204. https://doi.org/10.1038/s41565-022-01266-2PMC9974593.
50. Wu Z, Tang Y, Liu Y, Chen Z, Feng Y, Hu H, et al. Co-delivery of fucoxanthin and Twist siRNA using hydroxyethyl starch-cholesterol self-assembled polymer nanoparticles for triple-negative breast cancer synergistic therapy. J Adv Res. 2024. https://doi.org/10.1016/j.jare.2024.04.017.

Publisher's Note